

Insight into the physical processes that shape the metallicity profiles in galaxies

B. Tapia¹, P.B. Tissera^{1, 2}, E. Sillero³, C. Casanueva¹, S. Pedrosa⁴, L. Bignone⁴, R. Dominguez Tenreiro⁵ & N. Padilla¹

¹ *Instituto de Astrofísica, Pontificia Universidad Católica de Chile, Chile*

² *Centro de Astro-Ingeniería, Pontificia Universidad Católica de Chile, Chile*

³ *Instituto de Astronomía Teórica y Experimental, CONICET-UNC, Argentina*

⁴ *Instituto de Astronomía y Física del Espacio, CONICET-UBA, Argentina*

⁵ *Departamento de Física Teórica, Universidad Autónoma de Madrid, España*

Contact / brian.tapia@uc.cl

Resumen / Los perfiles radiales de abundancia en galaxias son el resultado de interacciones complejas entre una variedad de procesos físicos tales como *inflows/outflows* de gas, SN/AGN *feedback*, interacciones o fusiones de galaxias, etc. Modelos simples de formación *inside-out* predicen un gradiente negativo en la distribución radial de metales, pero observaciones muestran que, en perfiles de metalicidad de galaxias en el universo local, se encuentran significativas desviaciones a esta simple tendencia lineal. Usamos un *set* de simulaciones pertenecientes al proyecto CIELO para estudiar la forma de los perfiles de metalicidad en galaxias durante su proceso evolutivo. Dos eventos especiales fueron analizados y discutidos para ser presentados como contribución mural en contexto de la 63^a Reunión Anual de la AAA.

Abstract / Radial abundance profiles in galaxies are the result of the complex interplays between a variety of physical processes such as gas inflows/outflows, SN/AGN feedback, galaxy mergers and interactions, etc. Simple inside-out formation models predict a negative gradient in the radial distribution of metals, but observations have provided evidence that significant deviations from a simple negative trend are found in the metallicity profiles of galaxies in the local universe. We used a set of simulations from the CIELO project to study the shape of the metallicity profiles in galaxies during its evolutionary process. Two special events were analyzed and discussed to be presented as a poster contribution at 63^a *Reunión Anual de la AAA*.

Keywords / galaxies: abundances — galaxies: evolution — methods: numerical

1. Introduction

Chemical abundance profiles store information about the history of galaxy formation (Tinsley, 1980). These patterns and their evolution are the result of the complex interplays between a variety of physical processes such as gas inflows/outflows, SN/AGN feedback, galaxy mergers and interactions, etc (see, e.g. Maiolino & Mannucci, 2019). These processes can shape radial metallicity profiles (Tissera et al., 2019) generating different gradients and breaks (Diaz, 1989), even when an inside-out galaxy formation model predicts negative gradients as the central regions are enriched before galaxy outskirts (Searle, 1971; Peimbert, 1979). IFU observations in the past decade have provided evidence of such behaviour in nearby galaxies, finding a large variety of metallicity gradients and systematic deviations from a single linear profile (Belfiore et al., 2017; Sánchez-Menguiano et al., 2018).

We aim to reveal the relationships between the profile characteristics and the main events that participate in the formation of galaxies. To do this, we used a set of simulations of the Chemo-dynamic properties of galaxies and the cosmic web project, CIELO. We present the preliminary results of our work.

2. Simulations

Briefly, the CIELO suite is composed of zoom-in hydrodynamic simulations of different halos selected from a dark matter only run of a cosmological periodic cubic box of side length $L=100 \text{ Mpc } h^{-1}$, consistent with a Λ CDM universe model with $\Omega_0 = 0.317$, $\Omega_\Lambda = 0.6825$, $\Omega_B = 0.049$, $h = 0.6711$.

Galaxies are identified within the virial radius and the central ones are selected for analysis. We follow their merger trees to identify all accretion events. Then, for each selected galaxy in the redshift range $z = [0, 1.2]$, we calculate the metallicity radial profile of its star-forming gas, that mainly forms the disk component. We also calculate the stellar and gas mass, the star formation rate (SFR) and the half-mass radius (R_e) of each galaxy.

3. Estimation of the Metallicity Gradients and SFR

We identify the star-forming gas in each galaxy, filtering by temperature ($T < 20000 \text{ K}$) and circularity ($J_z/J_{\text{max}} > 0.5$) (Tissera et al., 2019). Then, we compute the oxygen abundance for the selected gas particles. Fig. 1 shows, in different epochs, the spatial distribu-

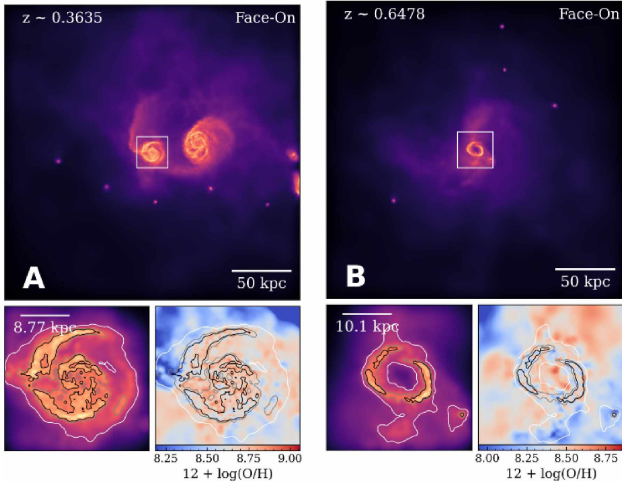


Figure 1: Face-on projections of the gas of galaxies during the events A (left) and B (right), centered in the main galaxy. Lower panels shows, respectively, density and oxygen abundance ($12 + \log(\text{O}/\text{H})$) maps in a $3R_e$ -side box. Three arbitrary density contours are shown to represent morphology.

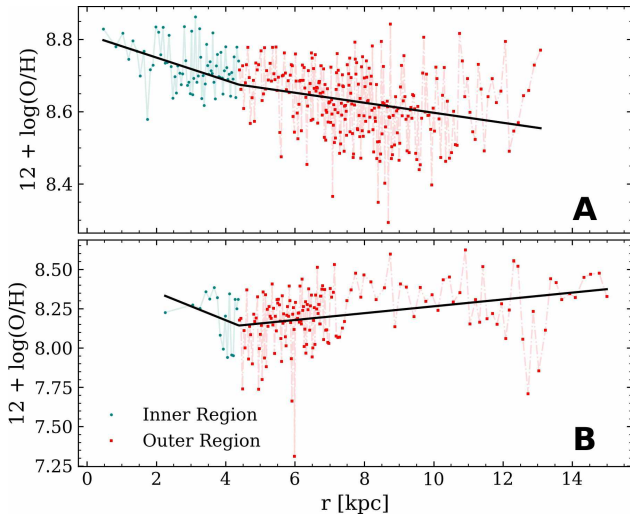


Figure 2: Metallicity profiles in moments A (upper panel) and B (lower panel). Data in inner and outer regions are plotted as blue dots and red squares, respectively. The fit in each profile is represented by a solid black line.

tion of this gas and its metallicity for one of the analyzed galaxies that we use as an example.

We build the oxygen abundance radial profile binning every 30 particles and make a piecewise linear fit to it, applying the least squares method. The adjustment break is set to $0.5 R_e$ and the continuity condition is imposed. Hereafter, we will refer to the areas bounded by this radius as the inner and outer regions. Examples of these profiles and fits can be seen in Figure 2. The metallicity gradient, $\nabla_{(\text{O}/\text{H})}$, is given by the slope of the linear function fitted to the metallicity profiles in each region.

In the defined zones, we also calculate the total rate of star formation. For this, we select the stars younger

than 0.5 Gyr and estimate the SFR as the total mass formed in that period. We repeat the process for the progenitors of each galaxy at $z = 0$ over 56 snapshots spanning from $z = 0$ to $z \sim 1.2$.

4. Evolution of the Metallicity Gradients

The evolution of the metallicity gradients and SFR are shown in the upper and middle panels of Figure 3 (respectively), for the inner (blue solid lines) and outer (red dashed-dotted lines) regions. As can be seen, the behavior of these gradients is fluctuating, with periods of strong variability at high redshift that tends to moderate for decreasing redshifts. The evolution of $\nabla_{(\text{O}/\text{H})}$ is different in the inner and outer regions, since the processes that affect the abundance profiles occur and impact at different spatial scales.

In an effort to identify these processes in the galaxy assembly history, we track the major galaxies that ended up merging with the central galaxy and its surviving satellites at $z = 0$. In the lower panel of Figure 3 we show, as a function of the redshift, the relative distance to the centers of mass of two galaxies, the most massive satellite (solid orange line) and a merger (dashed black line). We highlight two approximation events that coincide with the moments of the gas distribution, and profiles and fit shown in Figures 1 and 2, respectively.

Event A corresponds to the first pericenter, around the central galaxy, of its most massive satellite. Comparison with the previous moments shows that these passages cause a steeper gradient in the inner region while a shallower gradient in the outer region. The dilution of the metallicity near the rupture radius suggests that metal-poor gas has been accreted in the inner zone as gas falls into the potential well from the outside, due to loss of angular momentum caused by the interactions. This is also in agreement with an increase of the star formation rate in the inner regions.

Note that the galaxy that ends up merged also interacts with the central galaxy during event A, but it is important to clarify that most of its mass has already been increased by the latter, so the effects observed in the central galaxy are mainly caused by its satellite.

A major fly-by occurs just before event B. This close passage may have triggered an important burst of star formation in the inner region, as seen in Figure 3. As product of this burst, the SN feedback generate mass-loaded galactic winds that could heat and sweep the remaining gas towards the outer regions and concentrate it in a ring structure (see Figure 1). The contribution of metal-poor gas from the passing galaxy could decrease the metallicity inside the ring and this interaction may also have drive part of the internal gas, facilitating its re-accretion and/or redistribution. As a consequence, the R_{eff} of the central galaxy is higher, its inner median oxygen abundance is lower ($\text{Me}(12 + \log(\text{O}/\text{H})) \sim 8.22$ dex) and its $\nabla_{(\text{O}/\text{H})}$ is positive.

The B event occurred immediately after and corresponds to an interaction with a massive galaxy that ended up merging to the central one at $z \sim 0.15$. Here the observed internal $\nabla_{(\text{O}/\text{H})}$ variate from positive to negative as gas begins to fall back to the inner regions

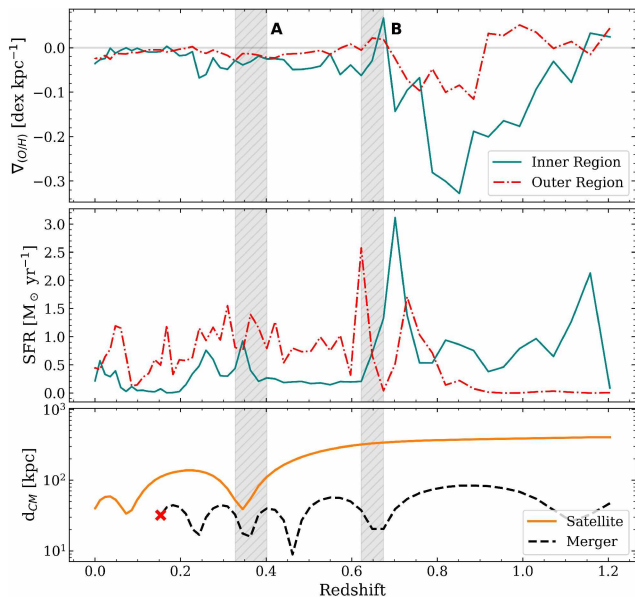


Figure 3: Evolution of the metallicity gradients (*upper panel*), SFR (*mid panel*), and relative distance of the interacting galaxies (*lower panel*) as a function of the redshift. Shaded regions correspond to interaction windows centered in events A and B.

and the induced star formation activity enrich the adjacent medium. Meanwhile, for the outer region, we observe that the effect of the current event produces a slightly more positive $\nabla_{(O/H)}$ by the gas accretion from the companion galaxy that also triggers the star forma-

tion in this region, as can be seen in Figure 3.

These examples illustrate how interaction affects the chemical distribution of gas along the galaxy, and hence, our estimation of the metallicity gradients. Of course, this kind of events could affect in different ways depending on their characteristics, and the gradients are not only affected by these mechanisms.

5. Conclusions/Future work

We found that the evolution of the metallicity gradients in a cosmological context is fluctuating, and the variations observed are mainly due to interactions between galaxies and their environment. We define inner and outer regions to understand the spatial scales of the processes that performed this variations. This analysis allow us to study the impact of the interactions to promote gas flows capable of modifying the star formation activity, and of diluting and/or redistributing the chemical abundances in different regions of the galaxy, resulting in metallicity profiles that exhibit different gradients and breaks.

References

- Belfiore F., et al., 2017, MNRAS, 469, 151
- Diaz A., 1989, Evolutionary phenomena in galaxies, 377
- Maiolino R., Mannucci F., 2019, A&A Rv, 27, 3
- Peimbert M., 1979, 22, 451
- Sánchez-Menguiano L., et al., 2018, A&A, 609, A119
- Searle L., 1971, ApJ, 168, 327
- Tinsley B.M., 1980, FCPH, 5, 287
- Tissera P.B., et al., 2019, MNRAS, 482, 2208